

Quadrupolar effects in the temperature dependence of the lattice parameters of $\text{HoP}_{1-x}\text{V}_x\text{O}_4$

S. Skanthakumar, C.-K. Loong, L. Soderholm, and J. W. Richardson, Jr.

Intense Pulsed Neutron Source and Chemistry Divisions, Argonne National Laboratory, Argonne, Illinois 60439

M. M. Abraham and L. A. Boatner

Solid State Division, Oak Ridge National Laboratory, Oak Ridge, Tennessee 37831

(Received 3 October 1994)

Powder-neutron-diffraction techniques have been used to investigate the temperature dependence of the structural properties of $\text{HoP}_{1-x}\text{V}_x\text{O}_4$ for x values of 0.0, 0.33, 0.52, 0.71, and 1.0. The diffraction data confirm the tetragonal zircon-type crystal structure for all of the samples in the temperature range between 12 and 300 K. The temperature dependence of the lattice parameters of the pure HoPO_4 and HoVO_4 , however, exhibits significant anomalies below about 100 K. In HoPO_4 , the lattice parameter a increases with decreasing temperature while c decreases. In HoVO_4 this behavior is reversed. These anomalies can be explained in terms of quadrupolar interactions of the Ho^{3+} ion with the crystalline lattice. In particular, the calculated quadrupole moments for HoPO_4 and HoVO_4 reproduce the observed temperature dependence and the inverse behavior. The anomaly in the thermal expansion is reduced in the case of the mixed phosphate vanadate materials ($0 < x < 1$) because of the competing Ho^{3+} quadrupole contributions.

I. INTRODUCTION

In crystalline solids containing heavy rare-earth elements with stable localized $4f$ -electronic orbitals, the wave functions of the rare-earth ions are primarily determined by the crystalline-electric fields imposed on the f electrons by the surrounding atoms. The magnetic properties (and optical properties for transparent materials) can often be satisfactorily described by means of a single-ion crystal-field model which represents the basis of an empirical Hamiltonian that employs a relatively limited number of crystal-field parameters. More-complex interactions between the f electrons and the host lattice as well as indirect exchange interactions among the f electrons via the crystalline medium can be treated by perturbation methods. Among the various crystal-field terms, the second-rank operator C_0^2 , which corresponds to the rare-earth electric-field quadrupole, is most sensitive to interactions with the environment. Some effects of quadrupolar interactions on various thermodynamic properties such as the thermal expansion, elastic constants, and Young's modulus in a variety of rare-earth materials have been investigated previously.¹⁻¹⁰

Ideally, an investigation of the effects of quadrupolar interactions on the thermodynamic properties would utilize a series of isostructural rare-earth compounds that fulfill the following requirements. First, insulating materials are preferred so that interactions with the lattice strains and phonons rather than conduction electrons are dominant. Second, the crystal structure should exhibit a unique axis of symmetry to which the anisotropic lattice properties and the projection of the rare-earth quadrupole moments can be referenced. Third, for simplicity, crystal structures accommodating only a single site-symmetry position for the rare-earth ions are preferred.

Fourth and finally, isostructural nonmagnetic compounds such as Y or Lu analogs should exist for the purpose of providing reference properties in the absence of rare-earth magnetic effects. The rare-earth orthophosphates, RPO_4 ($R = \text{Tb to Lu}$), and rare-earth orthovanadates, RVO_4 ($R = \text{all rare-earth elements except La}$) were determined to satisfy all of the above conditions, and therefore, they represent excellent candidate systems for the study of spin-lattice interactions due to quadrupolar effects.

Motivated by their importance in diverse areas such as laser/phosphor host media and Jahn-Teller-type phase transitions, we have recently initiated a systematic study of the $4f$ -electron crystal-field-level structure in the RPO_4 and RVO_4 systems by means of neutron spectroscopy and magnetic-susceptibility measurements.¹¹⁻¹⁶ We find that, despite the common tetragonal crystal structure and rare-earth site symmetry, the quadrupole-moment parameters B_0^2 of a given rare-earth phosphate and the corresponding vanadate are of opposite sign. This property gives rise to rare-earth ground-state wave functions of different symmetries. Consequently, a given RPO_4 and the corresponding RVO_4 often exhibit contrasting low-temperature magnetic behavior. In particular, HoPO_4 has a magnetic-doublet ground state consisting of a 98% $|8,7\rangle$ component, whereas HoVO_4 has a nonmagnetic singlet ground state containing an $\sim 90\%$ pure $|8,0\rangle$ component.¹²⁻¹⁶ These two compounds exhibit an "opposite" magnetic anisotropy at low temperatures, i.e., favoring an "easy magnetization axis" along the c direction for HoPO_4 as compared to an "easy plane" coinciding with the crystallographic a - b plane for HoVO_4 . At 1.4 K, indirect dipole-dipole interactions between the Ho moments apparently lead to long-range antiferromagnetic ordering with the moments parallel or antiparallel to the c axis.¹⁷ The Ho^{3+} ion in HoVO_4 has a

nonmagnetic ground state and, therefore, shows no ordering down to mK temperatures. Accordingly, in the mixed compound $\text{HoP}_{1-x}\text{V}_x\text{O}_4$, the overall anisotropy with respect to the c axis and the Ho quadrupole-moment-lattice interaction are expected to vary between the two limiting cases as x changes from 0 to 1.

In the present work, neutron-diffraction techniques are used to study the effects of Ho quadrupole-moment-lattice interactions on the thermal expansion coefficients in the mixed system $\text{HoP}_{1-x}\text{V}_x\text{O}_4$ (with $x = 0, 0.10, 0.33, 0.52, 0.71, 0.90$, and 1.0). In the end-member compounds HoPO_4 and HoVO_4 , the lattice parameters a and c show strong anomalies at temperatures below about 100 K. In HoPO_4 , a increases with decreasing temperature while c decreases with decreasing temperature, and the reverse behavior is observed for HoVO_4 . This anomalous temperature dependence diminishes as phosphorus is replaced by vanadium toward the $x = 0.5$ composition in $\text{HoP}_{1-x}\text{V}_x\text{O}_4$. No anomalous variation of the lattice parameters with temperature was observed in the pure end-member compounds LuPO_4 and LuVO_4 , thereby confirming the magnetic origin of the anomalies in the Ho system. This result is consistent with the temperature dependence of the quadrupole moments of the Ho^{3+} ions in HoPO_4 and HoVO_4 based on the crystal-field wave functions derived from previous neutron inelastic-scattering experiments.^{12,16}

II. EXPERIMENTAL DETAILS

Polycrystalline powder samples of $\text{HoP}_{1-x}\text{V}_x\text{O}_4$, LuPO_4 , and LuVO_4 employed in these investigations were prepared by a chemical coprecipitation technique described elsewhere.¹⁸ The neutron-diffraction experiments were performed using the General-Purpose Powder Diffractometer at the Intense Pulsed Neutron Source at Argonne National Laboratory. The samples were cooled by a closed-cycle helium refrigerator while sealed under a helium atmosphere in vanadium containers in order to enhance the thermal conduction at low temperatures. The data were collected at a mean detector angle of 148° , which corresponds to an instrumental resolution $\Delta d/d$ of about 0.0025. Data between the d spacings of 0.432 and 2.963 Å were analyzed using the Rietveld refinement technique.¹⁹ In the zircon-type

structure (space group $I4_1/amd$), the crystallographic sites of the R , M , and O atoms in RMO_4 ($R = \text{Ho, Lu}$; $M = \text{P, V}$) are $4a$, $4b$, and $16h$, and their coordinates are $(0, \frac{3}{4}, \frac{1}{8})$, $(0, \frac{1}{4}, \frac{3}{8})$, and $(0, y, z)$, respectively. The neutron coherent-scattering lengths used for Ho, Lu, P, V, and O in units of 10^{-12} cm^{-1} were 0.808, 0.730, 0.513, -0.038 , and 0.580, respectively. Since there is a large difference between the neutron-scattering lengths of phosphorus and vanadium, the relative (P/V) concentration in these samples can be accurately determined.

III. RESULTS AND DISCUSSION

The diffraction patterns of all of the $\text{HoP}_{1-x}\text{V}_x\text{O}_4$ samples confirm the existence of the single-phase, tetragonal zircon structure over the measured temperature range of 12 to 300 K.²⁰ For samples with mixed P and V, the structural analyses indicate a random substitution of P and V in the crystallographic site $4b$. The Rietveld-weighted R factors were between 5 and 7%. Refined room-temperature parameters and some of the interatomic distances are given in Table I. Using these results, empirical relationships between the structural parameters and the vanadium concentration x were obtained from a least-squares fit yielding the lattice constants and oxygen positions for $\text{HoP}_{1-x}\text{V}_x\text{O}_4$ given by the relationships

$$a = (6.885 + 0.238x) \text{ \AA} , \quad (1a)$$

$$c = (6.024 + 0.263x) \text{ \AA} \quad (1b)$$

and

$$y = 0.4242 + 0.0100x , \quad (2a)$$

$$z = 0.2165 - 0.0153x . \quad (2b)$$

In these materials, a Ho ion is surrounded by eight oxygen atoms, with four O at an equal distance denoted by $d_{\text{Ho-O1}}$ and the other four O at a second equal distance $d_{\text{Ho-O2}}$ (see Table I). Each set of four O ions forms a tetrahedron around a Ho ion, with one tetrahedron rotated relative to the other by 90° about the c axis. A phosphorus or vanadium atom is surrounded by a tetrahedron of oxygen ions with a distance denoted by $d_{(\text{P,V})-\text{O}}$ as given in Table I. The major change in interatomic distances with increasing V concentration occurs in $d_{(\text{P,V})-\text{O}}$,

TABLE I. The lattice constants, oxygen positional parameters, and the R-O and (P,V)-O nearest-neighbor distances for $\text{RP}_{1-x}\text{V}_x\text{O}_4$ ($R = \text{Ho}$ and Lu) at room temperature (296 K).

x	a (Å)	c (Å)	y	z	$d_{\text{Ho-O1}}$ (Å)	$d_{\text{Ho-O2}}$ (Å)	$d_{(\text{P,V})-\text{O}}$ (Å)
0.00	6.8842(1)	6.0255(1)	0.4246(2)	0.2150(2)	2.3047(12)	2.3771(11)	1.5400(11)
0.10(2)	6.9106(2)	6.0518(2)	0.4252(3)	0.2158(3)	2.3106(18)	2.3916(18)	1.5475(20)
0.33(1)	6.9580(1)	6.1048(1)	0.4270(2)	0.2125(2)	2.3102(12)	2.4004(11)	1.5813(11)
0.52(1)	7.0079(1)	6.1600(1)	0.4292(2)	0.2089(1)	2.3070(09)	2.4096(08)	1.6198(09)
0.71(1)	7.0540(1)	6.2117(1)	0.4313(2)	0.2056(2)	2.3035(11)	2.4205(10)	1.6542(10)
0.90(2)	7.0999(1)	6.2625(1)	0.4334(1)	0.2023(1)	2.2993(07)	2.4285(07)	1.6926(07)
1.00	7.1207(1)	6.2860(1)	0.4342(1)	0.2010(1)	2.2986(07)	2.4333(07)	1.7080(07)
LuPO_4	6.7967(2)	5.9593(3)	0.4269(2)	0.2154(2)	2.2615(14)	2.3502(13)	1.5327(14)
LuVO_4	7.0242(1)	6.2344(1)	0.4365(1)	0.1994(1)	2.2487(06)	2.4101(07)	1.7088(07)

while only a small change is observed in the Ho-O distances.

The variations of the lattice parameters a and c with temperature as determined for LuPO_4 and LuVO_4 are shown in Fig. 1. The thermal expansion follows a Debye-like temperature dependence, i.e., both a and c gradually decrease with decreasing temperature down to 12 K. These compounds serve as a nonmagnetic reference for the Ho(P,V)O_4 system since the $4f$ shell of the Lu^{3+} ions in Lu(P,V)O_4 is completely filled.

The temperature dependence of the lattice parameters a and c of HoPO_4 and HoVO_4 is shown in Fig. 2. At high temperatures (above 120 K), both materials show a thermal expansion that is similar to the lutetium analogs. Below 100 K, significant anomalies are evident for the pure HoPO_4 and HoVO_4 compounds. In the case of HoPO_4 , a increases with decreasing temperature while c decreases at a faster rate than that observed for LuPO_4 . This temperature-dependent behavior is reversed in HoVO_4 : i.e., a decreases with decreasing temperature while c increases. The fact that these anomalies are observed only in the magnetic materials and not in the nonmagnetic materials (e.g., LuPO_4 and LuVO_4) clearly indicates that they are magnetic in origin and involve unpaired $4f$ electrons.

The magnetic contribution to the thermal expansion as a function of temperature for HoPO_4 and HoVO_4 is shown in Fig. 3. This magnetic contribution to $\Delta a/a$ and $\Delta c/c$ was obtained by subtracting the corresponding values obtained using the nonmagnetic lutetium compounds. Here $\Delta l/l$ denotes $(l - l_{\text{rt}})/l_{\text{rt}}$ where l_{rt} is a room-temperature lattice parameter. These data clearly show that the anomalous thermal expansion in the a and c directions of HoVO_4 is opposite to that observed for HoPO_4 .

Understanding the magnetic origin of these anomalies requires a knowledge of the Ho^{3+} wave functions in both HoPO_4 and HoVO_4 . Both of these wave functions have been previously obtained by analyses of inelastic-neutron and magnetic-susceptibility data.^{12,16} The Ho^{3+} ions in both cases occupy a single site of D_{2d} symmetry, there-

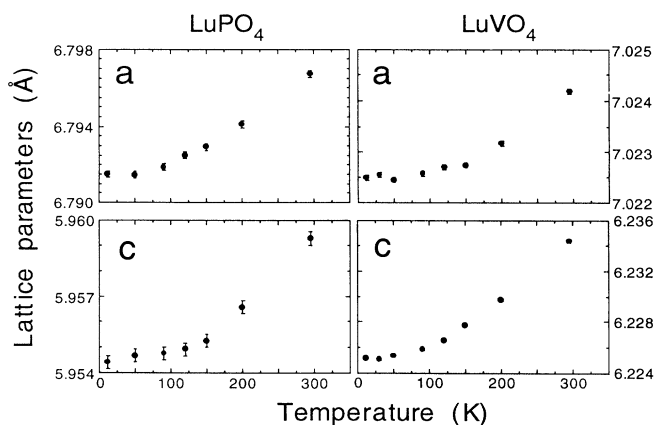


FIG. 1. The lattice parameters a and c of LuPO_4 and LuVO_4 as a function of temperature.

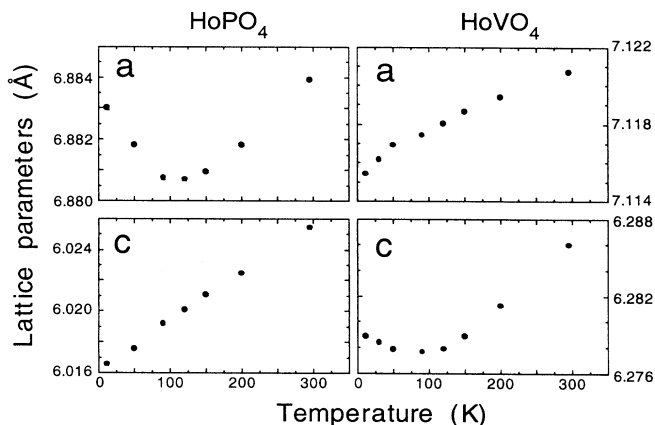


FIG. 2. The lattice parameters a and c of HoPO_4 and HoVO_4 as a function of temperature.

fore the crystal field splits the 5I_8 ground multiplet of the ion into nine singlets ($3\Gamma_1$, $2\Gamma_2$, $2\Gamma_3$, and $2\Gamma_4$) and four doublets ($4\Gamma_5$) and defines the “easy” direction for the magnetic moment. The rare-earth wave functions can be characterized by five crystal-field parameters B_0^2 , B_0^4 , B_0^6 , B_4^4 , and B_4^6 using a single-ion crystal-field model under the scheme of intermediate coupling.²¹ These parameters were obtained by fitting the observed neutron-magnetic-

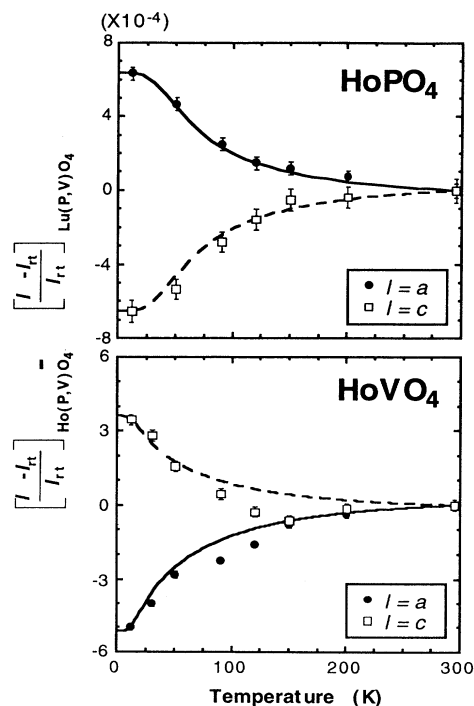


FIG. 3. The magnetic contribution to the relative change in the lattice parameters as a function of temperature for HoPO_4 and HoVO_4 . The magnetic contribution is obtained by subtracting the relative change in the lattice parameters of the corresponding lutetium compounds. The lines represent the calculated quadrupole moment of the Ho^{3+} ion normalized to the data at 12 K.

excitation spectra.

The important distinction between HoPO_4 and HoVO_4 lies in the sign difference in B_0^2 , which defines to the magnetic-anisotropy direction arising from the quadrupole moment.²² In HoPO_4 ,¹² the crystal-field parameter B_0^2 is 402 cm^{-1} , and the ground state of the Ho^{3+} ion is a Γ_5 doublet (containing about a 98% pure $|8,7\rangle$ component) with the magnetic-moment “easy” direction lying along the crystallographic c axis. The magnetic susceptibility is highly anisotropic at low temperatures. At 5 K, $\chi_{\parallel}/\chi_{\perp}$ is about 45 where χ_{\parallel} and χ_{\perp} are the magnetic susceptibilities parallel and perpendicular to the crystallographic c direction, respectively. In HoVO_4 ,¹⁶ the crystal-field parameter B_0^2 is -164 cm^{-1} . The ground state of the Ho^{3+} ion is a nonmagnetic Γ_1 singlet (containing about a 90% pure $|8,0\rangle$ component), and the magnetic moment “easy” direction is in the basal crystal plane. The magnetic susceptibility is also highly anisotropic, but unlike the case of HoPO_4 , $\chi_{\parallel}/\chi_{\perp}$ is about 0.021 at 10 K.

Since magnetization densities are connected to the $4f$ charge distributions, the large magnetic anisotropy observed at low temperatures indicates that the ground-state $4f$ charge distribution is highly aspherical in these materials. This asphericity can be expressed in terms of a quadrupole moment to first order. As the temperature increases, the anisotropic ground state becomes depopulated and the low-lying excited states become occupied, thereby reducing the asphericity of the $4f$ charge distribution. Consequently, if the $4f$ electrons are coupled to the crystalline lattice by virtue of a perturbation due to a quadrupolar interaction, the lattice properties should exhibit a temperature dependence that reflects the change in the $4f$ charge distribution as a function of temperature. The magnetic contribution to the temperature dependence of the lattice parameters in the linear-response approximation is simply proportional to the quadrupolar moment $Q(T)$ of the rare-earth ion¹⁻¹⁰

$$\frac{\Delta l}{l} \propto Q(T), \quad l=a \text{ or } c, \quad (3)$$

where

$$Q(T) \propto \frac{1}{Z} \sum \langle n | C_0^2 | n \rangle \exp(-E_n/k_B T). \quad (4)$$

Here Z is the partition function $Z = \sum \exp(-E_n/k_B T)$, $|n\rangle$ is the crystal-field-split state of the rare-earth ion with the quantization axis either parallel or perpendicular to the c axis, and C_0^2 is the quadrupolar operator. Equations (3) and (4) show that the magnetic contribution to the relative change in the lattice parameters has the same temperature dependence as the quadrupole moment.

The calculated temperature dependence of the quadrupole moment for HoPO_4 and HoVO_4 is compared with the experimental results in Fig. 3. The lines represent the calculated quadrupole moment normalized to the experimental data at 12 K. The results show a temperature

dependence of the electronic quadrupole moment consistent with the corresponding lattice parameters in both HoPO_4 and HoVO_4 . The calculated quadrupole moment in HoVO_4 is found to be opposite in sign to that of HoPO_4 . This explains the “reversed” behavior of the observed anomaly in the a and c lattice parameters between these two materials, i.e., anomalies in the temperature dependence of the lattice parameters can be explained by considering the rare-earth ion’s quadrupolar interaction with the crystalline lattice. In principle, the rare-earth quadrupole moment-lattice coupling also effects other physical properties of the lattice. An anomalous temperature dependence of the elastic constants and Young’s modulus has been reported previously for HoPO_4 and HoVO_4 .^{9,23}

The temperature dependence of the relative change in the lattice parameters of a and c for the $\text{HoP}_{1-x}\text{V}_x\text{O}_4$ ($0 \leq x \leq 1$) system is shown in Fig. 4. The magnitude of the anomaly in the temperature dependence of the lattice parameters is progressively reduced as x approaches to 0.5 from either end. In the mixed materials, the magnetization “easy” directions are frustrated by the opposing anisotropies, and the system is expected to behave like a random-anisotropy system similar to the case of $\text{DyP}_{1-x}\text{V}_x\text{O}_4$.^{24,25} For the same reason, the average quadrupole moment in the $1 < x < 0$ compounds is smaller in magnitude than those of the end-member materials. Hence, the quadrupolar effects on the anomalous temperature dependence of the lattice parameters are also expected to be reduced. The present neutron-diffraction data (Fig. 4) for the mixed $\text{HoP}_{1-x}\text{V}_x\text{O}_4$ materials are consistent with this interpretation.

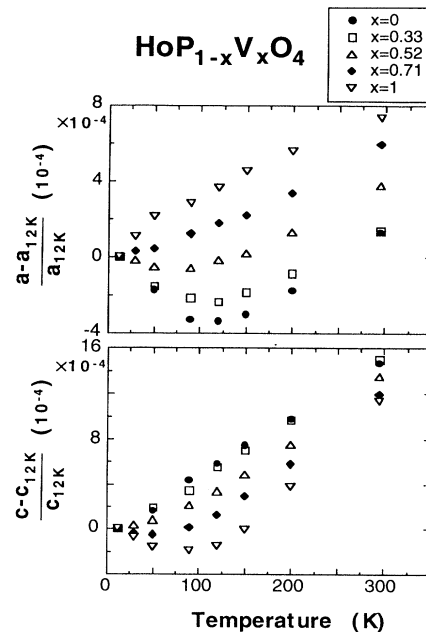


FIG. 4. The lattice parameters a and c of $\text{HoP}_{1-x}\text{V}_x\text{O}_4$ as a function of temperature.

ACKNOWLEDGMENTS

We thank S. Kern, J. Nipko, F. J. Rotella, U. Staub, and B. C. Chakoumakos for helpful discussions. Research at the Argonne National Laboratory and the

Oak Ridge National Laboratory was supported, respectively, by the Department of Energy, Office of Basic Energy Sciences under Contract No. W-31-109-ENG-38, and by Contract No. DE-AC05-84OR21400 with Martin Marietta Energy Systems, Inc.

-
- ¹M. E. Mullen, B. Lüthi, P. S. Wang, E. Bucher, L. D. Longinotti, J. P. Maita, and H. R. Ott, *Phys. Rev. B* **10**, 186 (1974).
²V. Dohm and P. Fulde, *Z. Phys. B* **21**, 369 (1975).
³L. Bonsall and R. L. Melcher, *Phys. Rev. B* **14**, 1128 (1976).
⁴P. S. Wang and B. Lüthi, *Phys. Rev. B* **15**, 2718 (1977).
⁵B. Lüthi and C. Lingner, *Z. Phys. B* **34**, 157 (1979).
⁶B. Lüthi and H. R. Ott, *Solid State Commun.* **33**, 717 (1980); H. R. Ott and B. Lüthi, *Z. Phys. B* **28**, 141 (1977).
⁷K. Andres, S. Darack, and H. R. Ott, *Phys. Rev. B* **19**, 5475 (1979).
⁸E. V. Sampathkumaran, I. Das, R. Vijayaraghavan, A. Hayashi, Y. Ueda, and M. Ishikawa, *Z. Phys. B* **92**, 191 (1993).
⁹V. I. Sokolov, Z. A. Kazei, and N. P. Kolmakova, *Physica B* **176**, 101 (1992); V. I. Sokolov, Z. A. Kazei, N. P. Kolmakova, and T. V. Solov'yanova, *Zh. Eksp. Teor. Fiz.* **99**, 945 (1991) [*Sov. Phys. JETP* **72**, 524 (1991)].
¹⁰P. Morin and D. Schmitt, in *Ferromagnetic Materials*, edited by K. H. J. Buschow and E. P. Wohlfarth (North-Holland, Amsterdam, 1990), Vol. 5, p. 1.
¹¹C.-K. Loong, L. Soderholm, M. M. Abraham, L. A. Boatner, and N. M. Edelstein, *J. Chem. Phys.* **98**, 4214 (1993).
¹²C.-K. Loong, L. Soderholm, J. P. Hammonds, M. M. Abraham, L. A. Boatner, and N. M. Edelstein, *J. Phys. Condens. Matter* **5**, 5121 (1993).
¹³C.-K. Loong, L. Soderholm, J. S. Xue, M. M. Abraham, and L. A. Boatner, *J. Alloys Compounds* **207-208**, 165 (1994).
¹⁴C.-K. Loong, L. Soderholm, G. L. Goodman, M. M. Abraham, and L. A. Boatner, *Phys. Rev. B* **48**, 6124 (1993).
¹⁵C.-K. Loong, L. Soderholm, J. P. Hammonds, M. M. Abraham, L. A. Boatner, and N. M. Edelstein, *J. Appl. Phys.* **73**, 6069 (1993).
¹⁶S. Skanthakumar, C.-K. Loong, L. Soderholm, M. M. Abraham, and L. A. Boatner (unpublished).
¹⁷A. H. Cooke, S. J. Swithenby, and M. R. Wells, *J. Phys. C* **6**, 2209 (1973).
¹⁸M. M. Abraham, L. A. Boatner, T. C. Quinby, D. K. Thomas, and M. Rappaz, *Radioactive Waste Manage.* **1**, 181 (1981).
¹⁹H. M. Rietveld, *J. Appl. Crystallogr.* **2**, 65 (1969).
²⁰W. O. Milligan, D. F. Mullica, G. W. Beall, and L. A. Boatner, *Inorg. Chem. Acta* **70**, 133 (1983); B. C. Chakoumakos, M. M. Abraham, and L. A. Boatner, *J. Solid State Chem.* **109**, 197 (1994).
²¹H. M. Crosswhite and H. Crosswhite, *J. Opt. Soc. Am. B* **1**, 246 (1984); W. T. Carnall, G. L. Goodman, K. Rajnak, and R. S. Rana, *J. Chem. Phys.* **90**, 3443 (1989).
²²J. E. Greedan and V. U. S. Rao, *J. Solid State Chem.* **6**, 387 (1973).
²³T. Goto, A. Tamaki, T. Fujimura, and H. Unoki, *J. Phys. Soc. Jpn.* **55**, 1613 (1986).
²⁴A. J. Dirkmaat, D. Hüser, G. J. Nieuwenhuys, J. A. Mydosh, P. Kettler, and M. Steiner, *Phys. Rev. B* **36**, 352 (1987).
²⁵P. Kettler, M. Steiner, H. Dachs, R. Germer, and B. Wanklyn, *Phys. Rev. Lett.* **47**, 1329 (1981).